

# The cross-coupled Interferometer for gravitational wave detection

Guido Mueller<sup>‡</sup>

Department of Physics, University of Florida, Gainesville, FL, 32611-8440

**Abstract.** The cross-coupled Interferometer is a new design for interferometric gravitational wave detectors. Similar to the baseline gravitational wave detectors proposed for Advanced LIGO, it uses long arm cavities in which the signal is generated. The signal fields are then extracted from the arm cavities with an additional cavity behind the long arm cavities. The tuning of this signal extraction cavity and the parallel tuning of the signal recycling mirror can be used to optimize the peak frequency and the bandwidth of the detector independently. If we replace the signal recycling mirror by a small cavity, it is possible to amplify signals in two different frequency bands.

<sup>‡</sup> Correspondence should be send to [mueller@phys.ufl.edu](mailto:mueller@phys.ufl.edu)

## 1. Introduction

Gravitational waves are caused by the most violent processes in the universe such as supernovae, merging stars, and colliding black holes. Several large scale interferometric gravitational wave detectors like LIGO [1] will begin operation over the next few years and open a new exciting window to the universe. Current estimates for the strengths of gravitational waves require a strain sensitivity of at least  $10^{-21}/\sqrt{\text{Hz}}$ . Real astronomy, which requires some knowledge of the location of the source and the wave form, will not be possible without reaching strain sensitivities well below  $10^{-23}/\sqrt{\text{Hz}}$ . This can only be achieved if we are able to suppress technical noise sources and reach the fundamental limits of interferometry. In this letter I will describe a new design for a gravitational wave detector, the cross-coupled interferometer. This design has some advantages over the dual recycling design proposed as the next major upgrade of the LIGO detectors. In particular, it offers a better tunability and can be extended to a system in which the effective bandwidth of the detector is larger than in the proposed Advanced LIGO configuration.

The optical layout of LIGO can be summarized as a power-recycled, cavity-enhanced Michelson interferometer (see fig. 1). The light field passes through a partially transmissive mirror, the PR-mirror. The beam splitter splits it into two fields which propagate in perpendicular directions. These fields bounce off two 4 km long Fabry Perot cavities formed between the partly transmissive input test masses (ITMs) and the high reflective end test masses (ETMs). These reflected fields interfere again at the beam splitter. The interference at the working point is constructive in the direction back of the PR-mirror (the bright port) and destructive in the perpendicular direction (the dark port). The cavity enhanced Michelson interferometer acts therefore as a simple mirror and together with the PR-mirror it forms an additional cavity: the power recycling cavity. Gravitational waves will change the interference pattern at the beam splitter and will direct some light to the dark port.

A slightly different detector is under construction by a group of German and British scientists in Germany [2]. The GEO detector is also a power recycled Michelson interferometer but has no cavities in its arms. Instead, it has an additional mirror at the dark port. This signal recycling (SR) mirror can amplify the signal in the interferometer. The potential sensitivity is comparable to the sensitivity of the first LIGO configuration.

The proposed Advanced LIGO detector [3] merges the optical configuration of the GEO detector with the configuration of the LIGO-I detector [4]. It can be described as a dual-recycled, cavity-enhanced Michelson-interferometer (see fig. 1). Gravitational waves modulate the phase of the carrier fields inside the arm cavities. This adds signal sidebands to the carrier. The beam splitter separates the sidebands from the carrier. The amplitudes of the sidebands scale with the amplitude of the carrier in the arm cavities. The carrier amplitude is proportional to the amplitude gain in the arm cavities  $g_c$  and in the power recycling cavity  $g_p$ . The amplitudes of the sidebands are also proportional to the sideband gain in the interferometer. In a LIGO-I configuration this gain is given

by the frequency dependent amplitude gain  $g_s(f)$  in the arm cavities. This gain in a signal-recycled configuration depends on the tuning of the signal-recycling mirror. The differential phase sensitivity in both cases is:

$$\frac{\phi_{min}(f)}{\sqrt{Hz}} = \frac{1}{g_c g_p g_s(f) \sqrt{n_{in}}} =: \frac{1}{A_{GW}(f)} \quad (1)$$

where  $n_{in}$  is the power of the input beam measured in photons per second.

Compared to LIGO I (see fig. 2) the gain  $A_{GW}(f)$  in Advanced LIGO can either increase in a very small frequency band around DC ( $\phi = 0^\circ$ ) or decrease while the bandwidth increases ( $\phi = 180^\circ$ ). A tuning between these two extremes is most likely the best tuning. In that case, the signal recycling cavity reduces the gain of the signal in the arm cavities slightly and pushes the peak frequency into a higher frequency range. The disadvantages are a limited bandwidth and the fact that a detuned interferometer only amplifies one of the signal sidebands and not both. Another disadvantage is that the peak sensitivity can not be tuned independently from the bandwidth. Any change in the position of the SR-mirror will change both. In principle, this can be changed to some extent by an additional cavity at the dark port instead of a single mirror.

## 2. The cross-coupled Interferometer

The front part of the cross-coupled interferometer is very similar to the Advanced LIGO configuration (see fig. 3). It has a power recycling mirror, a beam splitter, arm cavities, and uses signal recycling in form of a small non-transmissive cavity. The field is resonant in the power recycling cavity and both arm cavities. The interference at the beam splitter is also constructive in the direction of the PR-mirror and destructive in the perpendicular direction. The ETMs in the cross-coupled interferometer have to be partially transmissive. The fields leaking through these mirrors are the input fields of a new cavity formed between the ETMs and a new partially transmissive corner mirror (CM). The geometry requires folded arm cavities to reduce the length of the corner cavity. The signal can either be measured directly behind CM by beating the signal against appropriate RF-sidebands or it can be measured after passing through an additional Mach Zehnder interferometer. The latter would separate the carrier from the signal sidebands. Again appropriate RF-sidebands [5] or a slightly detuned Mach-Zehnder and a DC-readout technique can be used [6].

The corner cavity can be described as a cavity with two inputs and two outputs (see fig.4). The input fields  $E_1$  and  $E_2$  are the fields inside the two long arm cavities. The fields inside the corner cavity are:

$$E_a = \frac{it_e (E_1 + r_c r_e e^{i\phi_c} E_2)}{1 - r_c^2 r_e^2 e^{i2\phi_c}} \quad (2)$$

$$E_b = \frac{it_e (E_2 + r_c r_e e^{i\phi_c} E_1)}{1 - r_c^2 r_e^2 e^{i2\phi_c}} \quad (3)$$

$t_e$ ,  $r_e$ ,  $t_c$  and  $r_c$  are the amplitude transmissivity and reflectivity of the ETMs and the corner mirror.  $\phi_c$  is the one-way phase shift inside the corner cavity. The output fields  $E_c$  and  $E_d$  are equal to  $E_a$  and  $E_b$  times  $t_c$  and an unimportant phase factor.

As the Michelson interferometer is held on a dark fringe, the round trip phase difference between the fields in the two arms at the beam splitter has to be a multiple of  $360^\circ$ . This requires that the phase difference of the carrier  $E_0$  at the ETMs in the two arm cavities is a multiple of  $180^\circ$ . In other words, the fields are either in-phase or  $180^\circ$  out of phase. Subsequently, the signal sidebands  $\epsilon_s$  in the arm cavities are either  $180^\circ$  out of phase or in-phase, respectively. For simplicity, we focus only on the first case. The second case requires only an additional  $180^\circ$ -phase shift in the corner cavity to give the same results.

$$E_{1,2} = E_0 \pm \epsilon_s \quad (4)$$

$$E_{a,b} = E_0 \frac{it_e (1 + r_c r_e e^{i\phi_c})}{1 - r_c^2 r_e^2 e^{i2\phi_c}} \pm \epsilon_s \frac{it_e (1 - r_c r_e e^{i\phi_c})}{1 - r_c^2 r_e^2 e^{i2\phi_c}} \quad (5)$$

A tuning of  $\phi_c$  can change the interference in the corner cavity from constructive for the carrier and destructive for the (low frequency) signals to destructive for the carrier and constructive for the (low frequency) signals. A constructive interference of the carrier will lower the storage time in the arm cavities and decrease the amplitude of the carrier up to several orders of magnitude. The obvious working point is where the interference is (close to) destructive for the carrier and constructive for the sidebands at an optimized signal frequency ( $\phi_c \approx 180^\circ$ ). Constructive interference of the sidebands extracts the signals from the long arm cavities.

The interferometer is most sensitive at a frequency which is determined by the round-trip phase shift in the whole interferometer. Tuning CM changes this frequency, but it also changes the signal build up in the corner cavity. As CM has a non-zero transmissivity, the frequency dependent build up turns into frequency dependent losses. Consequently, the signal gain and the resonance frequency both depend on the tuning of CM. This is exactly the same for detuned resonant sideband extraction in an Advanced LIGO configuration [4]. The tuning of an SR-mirror at the dark port also changes the frequency at which the interferometer is most sensitive. But because the transmissivity of the SR-cavity is zero (and we assume zero losses), this tuning does not change the bandwidth of the detector.

### 3. Sensitivity

The calculated sensitivity that will be used to compare the two configurations is limited only by shot noise. Neither thermal noise nor radiation pressure noise nor the fully quantized description of the input field [7] is included in the sensitivity curves. The input power for all tunings and configurations is adjusted such that the power inside the arm cavities is always the same. As a result, thermal noise and all other problems caused by the circulating power in the arm cavities should be equal. In some tunings, this

requires unrealistically large input powers. However, in all realistically useful tunings, the necessary input power in the cross-coupled interferometer would be no more than a factor two above the power used in the Advanced LIGO configuration. The ITMs are identical in both designs, and the power inside the power recycling cavity would also be very similar in all useful tunings. In addition, folded arm cavities are used to simulate the Advanced LIGO configuration. Throughout the paper the detection process itself is ignored and the fundamental optical phase sensitivity of idealized interferometers as described in Eq. 1 is used.

Fig. 5 shows  $A_{GW}(f)$  for three different tunings of the corner mirror. For these calculations the signal recycling cavity was replaced by a single SR-mirror with a reflectivity of one and tuned to dual recycling ( $\phi = 0$  in Fig. 2). As long as  $\phi_c$  is below  $160^\circ$  the gain function has a very sharp resonance at very low frequencies. Above  $160^\circ$  the transfer function broadens and the resonance moves to larger frequencies. This would result in sensitivities that are very similar to the sensitivities of the Advanced LIGO configuration shown in Fig. 2. A tuning of the signal recycling mirror will not change the bandwidth but will tune the instrument to different frequencies. This can be seen in Fig. 6 for the case where the CM-mirror is tuned to  $\phi_c = 180^\circ$ . For  $|\phi_s| < 160^\circ$ , the resonance frequency will stay around DC. Above  $|\phi_s| > 160^\circ$ , the resonance frequency changes very fast with  $\phi_s$  and can be tuned to any interesting frequency range. Generally speaking, a tuning of CM changes frequency and bandwidth, while a tuning of SR changes only the frequency. A tuning of both permits independent changes in bandwidth and frequency.

The phase shift in the signal recycling arm versus the peak frequency of  $A_{GW}(f)$  for a detuned CM-mirror ( $\phi_c = 182^\circ$ ) is shown in Fig. 7. If the peak frequency is chosen, for example, to be 500Hz, the signal recycling arm has to add a phase shift of  $-157^\circ$  to the sidebands. The dashed lines show the phase shift that an additional cavity at the signal recycling port adds to the sidebands. This line crosses the solid line at two frequencies. The interferometer will have two different peak frequencies, in this case  $-180$  Hz and 600 Hz.

The sensitivity for such a configuration is shown in Fig. 8 for different CM-parameters. For the curve  $X - IFO_1$  I used a CM with a reflectivity of 95% and a detuning of  $182^\circ$ , for  $X - IFO_2$  I used 99% and  $181^\circ$ . The first curve shows two frequency bands in which the detector reaches its peak sensitivity. The second curve shows a very flat portion in the interesting frequency region between 100 and 1000Hz.

#### 4. Summary

A gravitational wave detector in the cross-interferometer configuration can be optimized in frequency response and its bandwidth independently by tuning the position of the corner mirror and of the SR mirror. An additional cavity at the signal recycling port tailors the frequency response. It can be used to achieve good sensitivity in two different frequency bands or used to get a nearly frequency independent sensitivity.

Nevertheless, it is now well known that the interaction between radiation pressure noise and the suspended mirrors modify the sensitivity curves. In particular, it adds a second resonance frequency to the sensitivity curve of the Advanced LIGO configuration. Although the calculations have never been done, it is clear that a similar resonance will show up in the cross-interferometer. A cross-interferometer configuration could have three different resonances. It should be possible to tailor these resonances and achieve a frequency-independent and very broadband sensitivity curve.

The author thanks the University of Florida LOGO-group for their support. The author gratefully acknowledges the support of the National Science Foundation grant PHY-0070854.

## 5. References

- [1] A. Abramovici et al., “LIGO: the Laser Interferometer-Gravitational Wave Observatory”, *Science* **256**, 325-333 (1992)
- [2] H. Lück and the GEO 600 team, “The GEO 600 Project”, *Class. Quantum Grav.* **14**, 1471-1476 (1997)
- [3] E. Gustafson et al., “LSC white paper on detector research and development”, LIGO Document Center T990080-00-D (1999)
- [4] Jun Mizuno, “Comparison of Optical Configurations for Laser-Interferometric Gravitational-Wave Detectors”, PhD thesis, University of Hannover, Germany (1995).
- [5] R.W.P. Drever, J.L. Hall, F.V. Kowalski, J. Hough, G.M. Ford, A.J. Munley, and H. Ward, *Appl. Phys. B* **31**, 97 (1983)
- [6] Ken Strain, Peter Fritschel, (private communication). A series of papers discussing length sensing and control aspects of Advanced LIGO is in preparation. In the mean time the author suggest the following theses: Daniel Shaddock, Australian National University (2001), James Mason, California Institute of Technology (2001), Thomas Delker, University of Florida (2001).
- [7] A. Buonanno and Yanbei Chen, “Quantum noise in second generation, signal-recycled laser interferometric gravitational-wave detectors”, *Phys. Rev. D* **64** (2001)

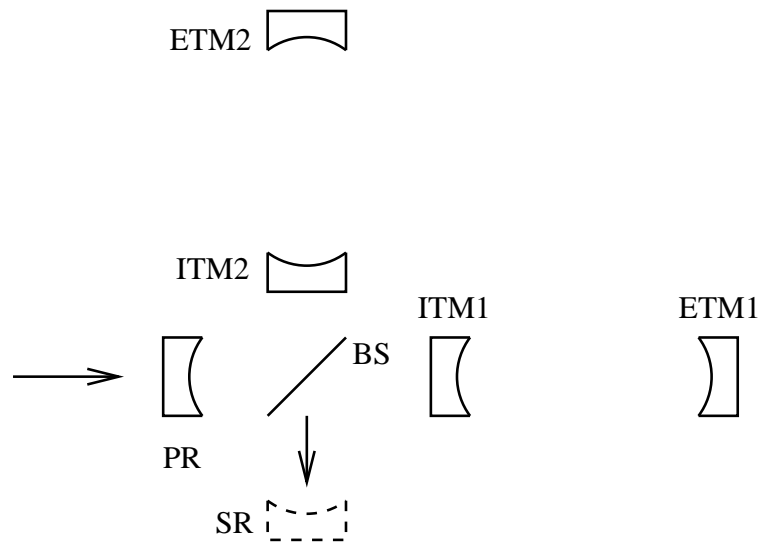


**Figure 1.** The LIGO configuration consists of a power recycling mirror (PR), a beam splitter (BS), and two arm cavities formed between the partially transmissive input test masses (ITM<sub>x</sub>) and the highly reflective end test masses (ETM<sub>x</sub>). The proposed Advanced LIGO configuration has an additional partially transmissive mirror at the dark port: the signal recycling mirror (SR).

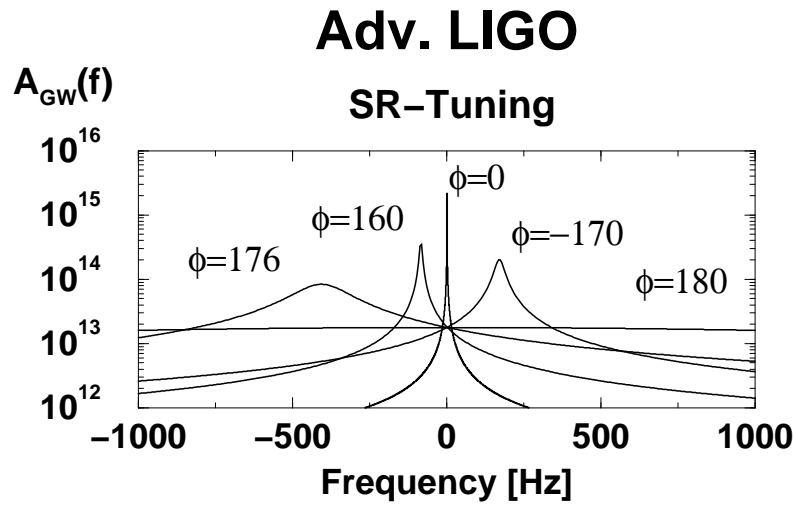


**Figure 2.** The transfer function for the signal sidebands in the proposed Advanced LIGO configuration for various tunings ( $\phi$ ) of the signal recycling mirror.  $\phi = 0^\circ$  is undetuned signal recycling.  $\phi = 180^\circ$  is undetuned resonant sideband extraction. The peak frequency and the bandwidth change with the tuning of the signal recycling mirror. Reflectivities of the mirrors:  $R_{PR} = 0.91$ ,  $R_{ITM_x} = 0.995$ ,  $R_{ETM_x} = 1$ ,  $R_{SR} = 0.97m$ . The arm cavities are 4 km long. Input Power: 76.3 W

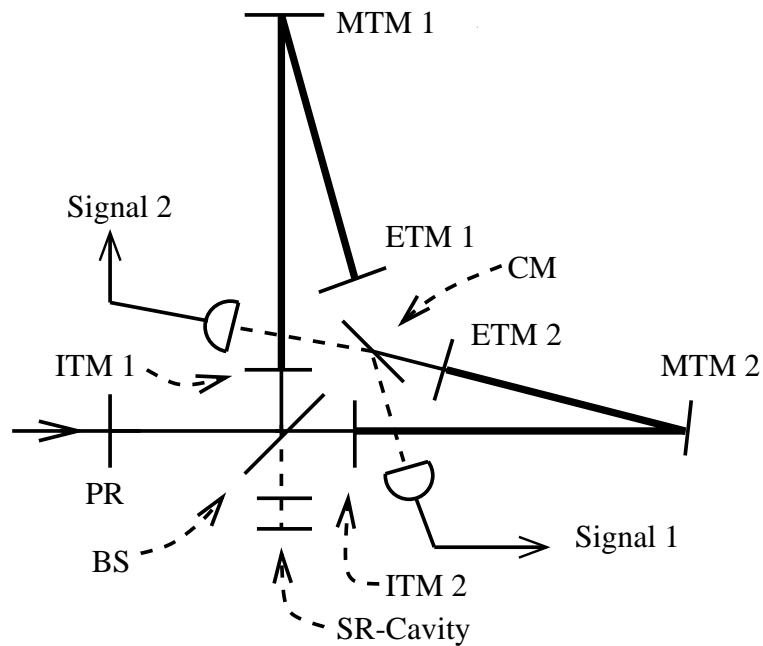


**Figure 3.** The cross-coupled interferometer consists of a power recycling mirror (PR), a beam splitter (BS), two folded arm cavities formed between the partially transmissive input test masses (ITM<sub>x</sub>), the highly reflective middle test masses (MTM<sub>x</sub>), and the partially transmissive end test masses (ETM<sub>x</sub>). The corner mirror and the ETMs form a new cavity that extracts the signal from the arm cavities. The signal recycling cavity (SR-cavity) closes the dark port.

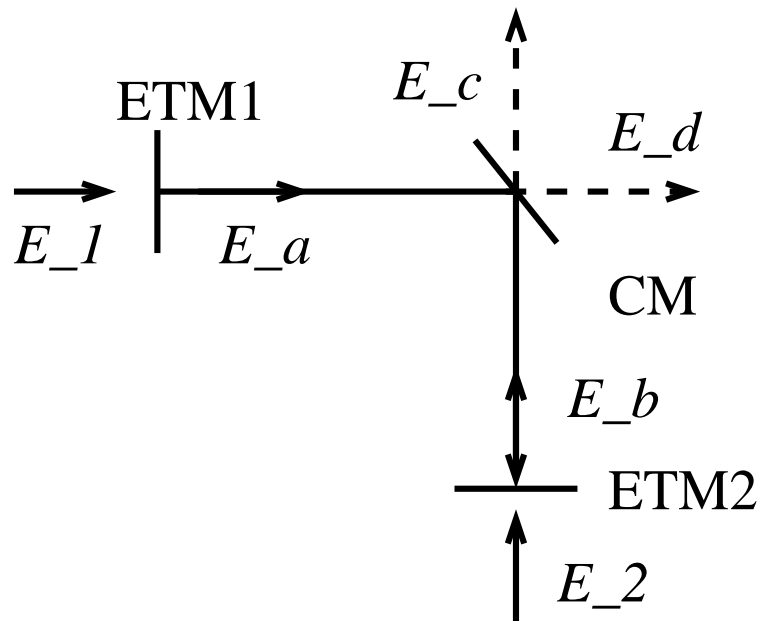


**Figure 4.** The fields in the long arm cavities  $E_1$  and  $E_2$  are the input fields of the corner cavity. The fields in this cavity are  $E_a$  and  $E_b$  and the output fields are  $E_c$  and  $E_d$ .

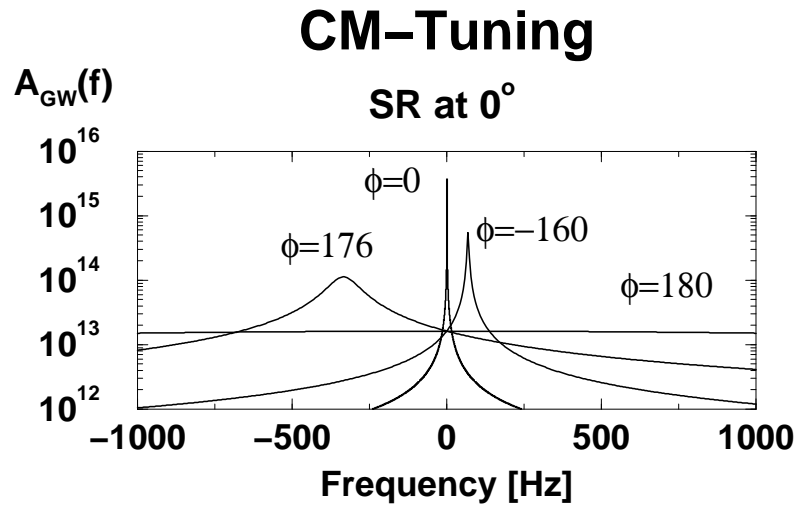


**Figure 5.** The transfer function of the signal sidebands for three different positions of the corner mirror. The graph for the 0° tuning shows a very sharp resonance at very low frequencies. This is a typical transfer function for all tunings below 160°. The graph -178° shows typical broad resonances at larger frequencies, while 180° is again similar to resonant sideband extraction. Note that the input power has to be adjusted to achieve the same power in the arm cavities. Reflectivities of the mirrors:  $R_{PR} = 0.92$ ,  $R_{ITM_x} = 0.995$ ,  $R_{ETM_x} = 0.996$ ,  $R_{MTM_x} = 1$ ,  $R_{SR} = 1m$ ,  $R_{CM} = 0.98$ . The arm cavities are 4 km long. Input Powers vary from: 96 W for  $\phi = 180^\circ$  to 6.9 GW (!) for  $\phi = 0^\circ$ .

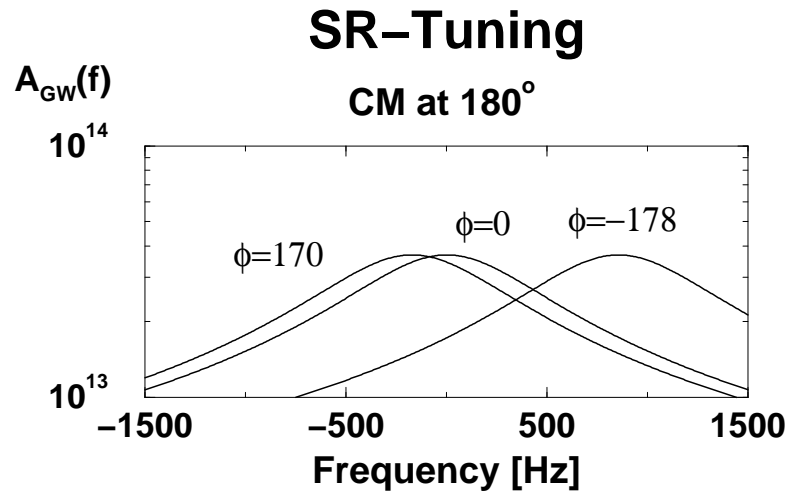


**Figure 6.** The transfer function of the signal sidebands for three different positions of the SR mirror. Note that the width of the resonance does not depend on that position. Thus, this can be used to tune the frequency of the detector without changing the bandwidth. Essential Parameters: Reflectivities of the mirrors:  $R_{PR} = 0.92$ ,  $R_{ITMx} = 0.995$ ,  $R_{ETMx} = 0.996$ ,  $R_{MTMx} = 1$ ,  $R_{SR} = 1m$ ,  $R_{CM} = 0.98$ . The arm cavities are 4 km long. Input Power: 96 W.

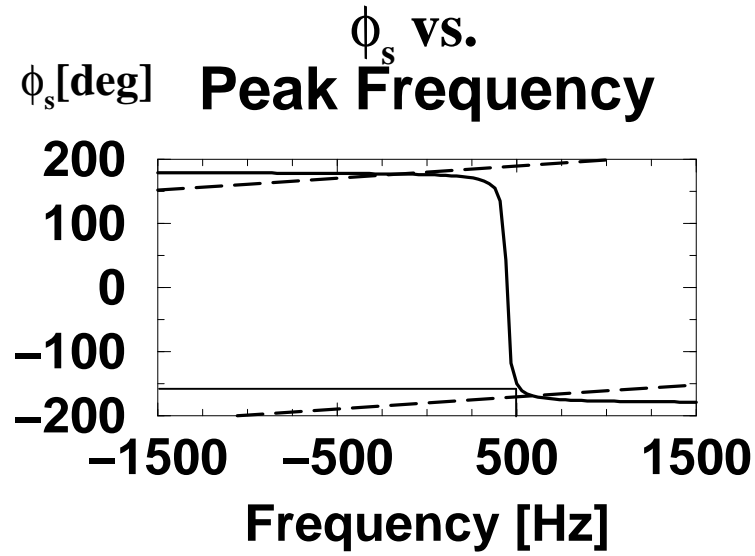


**Figure 7.** The phase shift in the SR-arm versus the peak frequency of  $A_{GW}(f)$  for a detuned CM-mirror  $\phi_{CM} = 182^\circ$  (solid line). For a peak frequency of 500 Hz the phase shift has to be  $-157^\circ$ . The dashed line shows the phase shift introduced by an additional small cavity in the dark port. The interferometer will built up the signal at all frequencies where the lines cross each other.

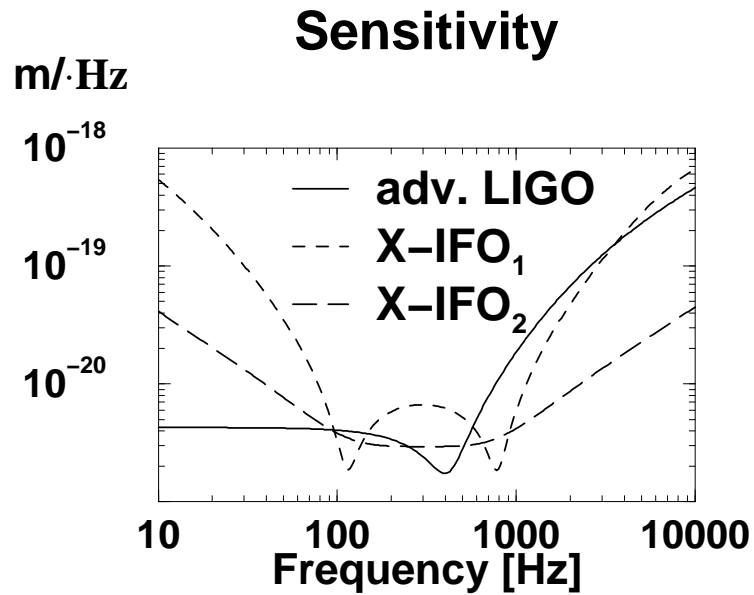


**Figure 8.** The sensitivity of the cross-coupled interferometer compared with the sensitivity of Advanced LIGO for two different tunings. In both configurations a DC-readout technique is used. The corner mirror in  $X - IFO_{1(2)}$  has a reflectivity of 99% (95%) and is detuned to  $91^\circ$  ( $90.5^\circ$ ). The intensities in the arm cavities were in all three cases the same. Parameters same as in fig. 2 and fig. 5, except that the SR-mirror is replaced by a cavity with an input mirror with  $R = 0.995$ .